



HAL
open science

Microwave evaluation of $\text{Pb}(0.4)\text{Sr}(0.6)\text{TiO}(3)$ thin films prepared by magnetron sputtering on silicon : performance comparison with $\text{Ba}(0.3)\text{Sr}(0.7)\text{TiO}(3)$ thin films

Freddy Ponchel, X. Lei, Denis Remiens, Gang Wang, X. Dong

► To cite this version:

Freddy Ponchel, X. Lei, Denis Remiens, Gang Wang, X. Dong. Microwave evaluation of $\text{Pb}(0.4)\text{Sr}(0.6)\text{TiO}(3)$ thin films prepared by magnetron sputtering on silicon : performance comparison with $\text{Ba}(0.3)\text{Sr}(0.7)\text{TiO}(3)$ thin films. *Applied Physics Letters*, 2011, 99, pp.172905-1-3. 10.1063/1.3656065 . hal-00783535

HAL Id: hal-00783535

<https://hal.science/hal-00783535>

Submitted on 27 May 2022

HAL is a multi-disciplinary open access archive for the deposit and dissemination of scientific research documents, whether they are published or not. The documents may come from teaching and research institutions in France or abroad, or from public or private research centers.

L'archive ouverte pluridisciplinaire **HAL**, est destinée au dépôt et à la diffusion de documents scientifiques de niveau recherche, publiés ou non, émanant des établissements d'enseignement et de recherche français ou étrangers, des laboratoires publics ou privés.

Microwave evaluation of $\text{Pb}_{0.4}\text{Sr}_{0.6}\text{TiO}_3$ thin films prepared by magnetron sputtering on silicon: Performance comparison with $\text{Ba}_{0.3}\text{Sr}_{0.7}\text{TiO}_3$ thin films

Cite as: Appl. Phys. Lett. **99**, 172905 (2011); <https://doi.org/10.1063/1.3656065>

Submitted: 25 July 2011 • Accepted: 06 October 2011 • Published Online: 27 October 2011

F. Ponchel, X. Lei, D. Rémiens, et al.



View Online



Export Citation

ARTICLES YOU MAY BE INTERESTED IN

[Aligned and exchange-coupled FePt-based films](#)

Applied Physics Letters **99**, 172504 (2011); <https://doi.org/10.1063/1.3656038>

[Current suppression and harmonic generation by intense terahertz fields in semiconductor superlattices](#)

Journal of Applied Physics **82**, 718 (1997); <https://doi.org/10.1063/1.365604>

[Low-temperature admittance measurement in thin film amorphous silicon structures](#)

Journal of Applied Physics **82**, 733 (1997); <https://doi.org/10.1063/1.365607>

Lock-in Amplifiers
up to 600 MHz



Zurich
Instruments



Microwave evaluation of $\text{Pb}_{0.4}\text{Sr}_{0.6}\text{TiO}_3$ thin films prepared by magnetron sputtering on silicon: Performance comparison with $\text{Ba}_{0.3}\text{Sr}_{0.7}\text{TiO}_3$ thin films

F. Ponchel,^{1,a)} X. Lei,² D. Rémiens,¹ G. Wang,² and X. Dong²

¹*Institute of Electronics, Microelectronics and Nanotechnology (IEMN) – DOAE, UMR CNRS 8520, Université des Sciences et Technologies de Lille, 59652 Villeneuve d'Ascq Cedex, France*

²*Key Laboratory of Inorganic Functional Materials and Devices, Shanghai Institute of Ceramics, Chinese Academy of Sciences, 1295 Dingxi Road, Shanghai 200050, People's Republic of China*

(Received 25 July 2011; accepted 6 October 2011; published online 27 October 2011)

$\text{Pb}_{0.4}\text{Sr}_{0.6}\text{TiO}_3$ (PST) thin films were deposited on high resistivity silicon substrate by radio frequency magnetron sputtering. A pure perovskite phase was obtained at a low post annealing temperature of 650 °C. The relative dielectric constant, loss factor, tunability, and figure of merit were determined over a large frequency range of 1 GHz to 60 GHz. A large tunability about 60% and a relatively low loss of 16% at 60 GHz were obtained. PST is an alternative material for microwave agile devices integrated with silicon and this is discussed from the standpoint of monolithic integration with a low thermal budget. © 2011 American Institute of Physics. [doi:10.1063/1.3656065]

Ferroelectric thin films such as $\text{Pb}(\text{Zr},\text{Ti})\text{O}_3$ (PZT), $\text{SrBi}_2\text{Ta}_2\text{O}_9$ (SBT), and $(\text{Ba},\text{Sr})\text{TiO}_3$ (BST) are currently used for tunable capacitor structures due to a strong variation of their relative dielectric constant under applied dc electric voltage, i.e., large electric-field-dependent tunability.¹ Many devices have been intensively studied and fabricated for different applications: tunable microwave devices/radio frequency components and power-supply decoupling.^{2,3} Among the various ferroelectric films, BST thin film is the most promising material for micro wave tunable capacitors due to its high dielectric constant, high tunability and its paraelectricity at normal operating temperatures. Although pure BST material presents a large loss factor, typically 10% at 60 GHz, which impacted on the device's figure of merit (FOM). For monolithic Si—integration with BST, post annealing at a temperature of around 750 °C, can damage electrodes, barrier metals, and contacts. Some authors have shown that the tunability of $\text{Pb}_{0.4}\text{Sr}_{0.6}\text{TiO}_3$ (PST) can be, depending on the Pb/Sr ratio, higher than BST and the loss factor stays relatively low.⁴

In this paper, we present the results of characterization of dielectric properties, relative dielectric constant, loss factor and tunability of PST films over large frequency range. For the Pb/Sr ratio of about 40/60, the tunability of the PST attained a maximum value; the target (PST ceramic) contains 25 wt. % of lead and 6 wt. % of strontium excess.⁵ The films were deposited by radio frequency magnetron sputtering onto high resistivity silicon (HRSi) substrates. The depositions were made *ex-situ* (without annealing the substrate during the growth) and so the as-grown films were amorphous. A post annealing temperature of 650 °C is sufficient to obtain a pure perovskite structure without parasitic phases. The details of the sputtering, post annealing conditions, and film composition are given in Ref. 6. A typical x-ray diffractogram is presented in Figure 1. The film thickness is 150 nm

(this will be discussed later) with a very thin TiO_x buffer layer. We have shown previously that the presence of a TiO_x buffer layer (3 nm thick) improves the BST crystallisation.⁷ For PST films, as presented in Figure 1, no effect was observed, a more complete study is necessary. The films are polycrystalline with a preferred (110) orientation. The microstructure of the PST films deposited on HRSi, obtained using scanning electron microscopy (SEM), is shown in Figure 1 (insert). The film is smooth and very dense; no cracks appear to be present. The grains sizes are very large, completely different to those measured for PST deposited on platinum.

To determine the electric properties (relative permittivity, loss factor, and tunability) of PST in the hyper-frequency domain, we used a developed process involving a coplanar waveguide with a 1 μm slot width and Figure 2(a) shows a 3D-scheme of this waveguide on PST film.^{8,9} This method was initially optimized for the BST thin film ($\epsilon'_{\text{BST}} \approx 300$),

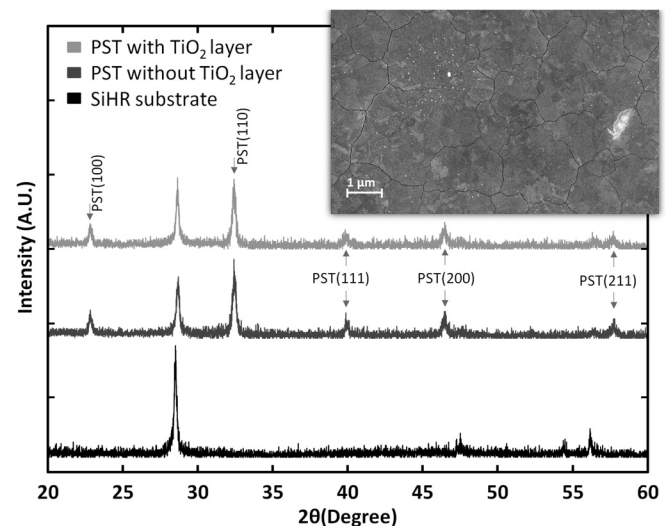


FIG. 1. X-ray diffraction layer patterns of PST films deposited on HRSi with a post annealing temperature of 650 °C. The inset shows a SEM view of the sample with buffer layer (corresponding to the light black line).

^{a)}Author to whom correspondence should be addressed. Electronic mail: freddy.ponchel@univ-lille1.fr.

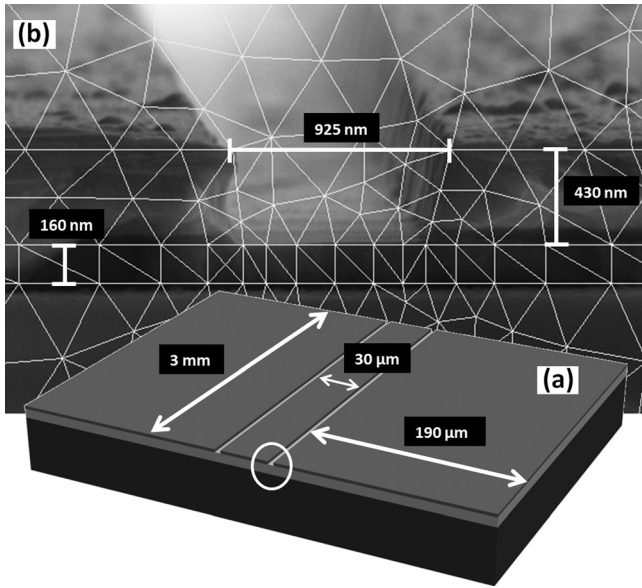


FIG. 2. (a) 3D schematic of the $1\ \mu\text{m}$ slot width coplanar waveguide (b): Meshed SEM view on one of the slots of the coplanar structure tested.

so it is necessary to take some precautions before quantifying this with PST. Indeed, for PST thin films, our measurements at low frequencies show a permittivity of between 450 and 550.⁷ Equation (1) describes the qualitative behavior of the attenuation constant α ($\gamma = \alpha + j\beta$).

$$\alpha^2 = \frac{2\pi^2 \epsilon_e'}{\lambda_o^2} \left(\sqrt{1 + \left(\frac{\lambda_o^2}{2\pi^2 \delta_e^2 \epsilon_e'} + \frac{\epsilon_e''}{\epsilon_e'} \right)^2} - 1 \right). \quad (1)$$

The subscript “e” refers to effective parameters, i.e., they depend on both the physical characteristics and topological characteristics of each region (substrate, electrode, PST, and air). ϵ_e' is the relative effective permittivity, δ_e is the effective skin depth (δ_e is a function of the effective conductivity σ_e), μ_e is the effective permeability, λ_o is the wavelength in vacuum, and f is the frequency. When $\epsilon_e'' > 0$ and/or $\sigma_e > 0$, the effective permittivity ϵ_e' acts as an amplifier of the waveguide losses. This is the main effect that we must take into account when the material characteristics are to be determined. Indeed, to perform the measurement up to 60 GHz, we must ensure that the parameters S_{ij} of an entire structure is not less than -35 dB at 60 GHz; this value corresponds to our template that takes into account the limitations of our vector network analyzer (VNA). Under these conditions, two solutions are possible. First, to increase the finger gap between the electrodes. However, as consequence, the applied DC electric field magnitude and tunability measurement are lowered. Second, to decrease the thickness of the film but this result in increasing mesh density and decreasing mesh quality. Concerning mesh density, it has a strong dependence on the thickness of the ferroelectric film. Really, VNA is not the only limiting factor, our bespoke software, based on a two-dimensional vector finite element method (2D VFEM) presents also some limitations. It is imperative to define the maximum film thickness that ensures a correct measurement and simultaneously minimizes the mesh density for the computational phase. We verified that the

simulation is possible as long as the layer thickness is not less than 130 nm. Taking into consideration all these limitations, we decided to maintain a DC electric field at 300 kV/cm (as for BST films) and to fix the PST film thickness at 150 nm. Figure 2(b) shows the final structure observed by SEM.

All the measurements are performed at ambient temperature using an Agilent E8361A PNA Microwave Network Analyzer coupled to a Cascade Microtech ground-signal-ground probe station. The scattering parameters are measured in the 1 to 60 GHz frequency band. Note that with this PNA, there is a measurement uncertainty of about 0.15–0.2 dB on the dynamic range (0 to -35 dB). This implies a relative uncertainty on $\tan \delta$ of approximately 2% while ϵ' determination is always better than 1%. For DC electric field control, we used an Agilent E5263A 2-Channel High Speed Source Monitor Unit, driven by IC-CAP device modelling software v2009. The bias voltage is swept between $+30$ V and -30 V. After extraction, we obtain the complex permittivity, i.e., the dielectric constant and the loss tangent under the DC applied voltage. The tunability is defined as $\{(\epsilon'(0) - \epsilon'(E_{max})) / \epsilon'(0)\} * 100\%$, where $\epsilon'(0)$ and $\epsilon'(E_{max})$ are the permittivity of PST film at zero and maximum applied voltage, respectively. With or without an external DC electric field, the relative dielectric permittivity is continuously diminishing as shown in Figure 3(a). At zero DC bias, it has a value of 390 at 1 GHz and reaches 350 at 60 GHz. The loss tangent ($\tan \delta$) increases with frequency and evolves from 0.017 to 0.16 at 1 GHz and 60 GHz, respectively (Figure 3(a)). The losses for PST films are of the same order as that for BST (0.11 at 60 GHz). A

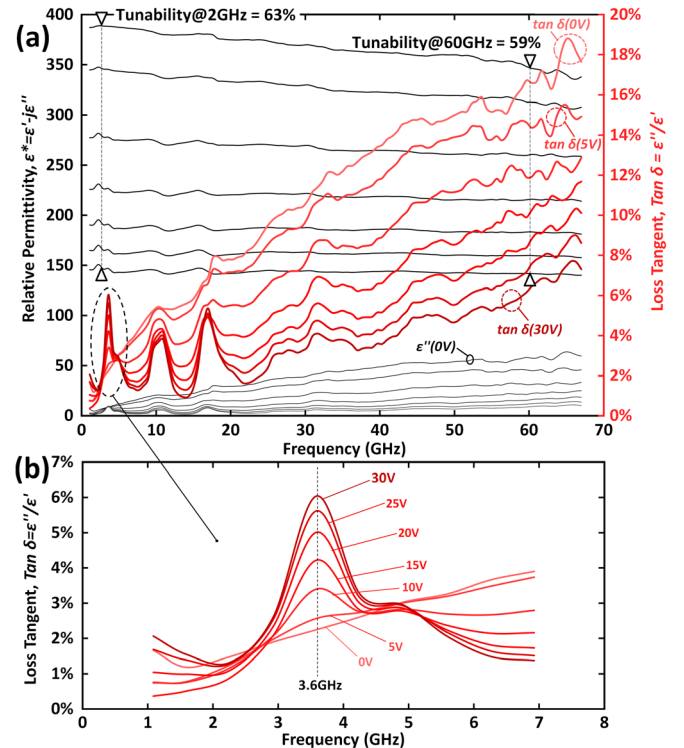


FIG. 3. (Color online) (a) Frequency behaviour of the complex permittivity ($\epsilon^* = \epsilon' - j\epsilon''$) and loss tangent ($\tan \delta = \epsilon''/\epsilon'$) of a $0.16\ \mu\text{m}$ thickness PST layer deposited on a $600\ \mu\text{m}$ HRSi substrate. (b): Loss tangent between 1 GHz and 7 GHz. In this frequency range, a resonant absorption peak was observed as a function of the DC bias voltage.

TABLE I. Synthesis of BST and PST results: comparison of dielectric characteristics at 1 GHz and 60 GHz.

Frequency (GHz)	BST		PST	
	1	60	1	60
$\epsilon'(0 \text{ kV/cm})$	296.6	284.3	387.0	346.4
$\epsilon'(300 \text{ kV/cm})$	198.8	196.7	145.5	140.1
$\tan \delta$ (%)	1.4	10.5	1.7	16.4
Tunability (%)	33.0	29.4	62.8	59.3
FOM		2.8		3.6

strong variation of the relative permittivity and loss factor with DC voltage at different frequencies are shown clearly in Figure 3(a). The tunability reaches very high value (63% at 1 GHz) and stays near constant even at very at frequency (59% at 60 GHz). Such a result is also observed on BST films but a factor of 2 is measured for the tunability of PST. The resonant absorption peaks in the frequency dependent loss tangent are observed as a function of the DC bias voltage, as shown in Figure 3(a), at 3.5 GHz, 10 GHz, and 17 GHz. The details of this behaviour are presented in Figure 3(b) for resonance absorption at 3.5 GHz. The loss increases when the DC applied electric field increases, typically under 30 V, we obtain a loss of 6% in comparison with a loss of 2% at 0 V. This resonance effect has been observed by some authors and explained by electrostriction and piezoelectric effects.¹⁰ The extensive transformation of microwave signals takes place at acoustic resonances, where the length between the electrodes is a multiple of the acoustic half-wavelengths, which leads to sharp peaks in the frequency dependent loss tangent. The acoustic resonance frequencies are determined by the acoustic velocities in the thin films which form the structure. A model that explains this particular effect has been developed by Lakin *et al.*¹¹ Table I compares our results on relative permittivity, losses, tunability, and FOM for polycrystalline BST and polycrystalline PST. The FOM is defined as $\{Tunability(60 \text{ GHz}, E = 30 \text{ V}) / \tan \delta(60 \text{ GHz}, E = 0 \text{ V})\}$. Even if the losses are little higher for PST, it is evident that this material presents great potential for agile microwave devices. Figure 4(a) summarizes the performance of PST films in terms of tunability, and we represent within this figure the results obtained with our BST films. From our measurements and dedicated software, we have deduced the characteristic impedance (Z_c), which is related to the tunability of the dielectric permittivity (Figure 4(b)). At 60 GHz, the variation of Z_c is about 36% (under 300 KV/cm DC electric field) for PST and only 19% for BST films. This result is very important to realise adaptive impedances at very high frequencies and can be used to optimize for tunable impedance matching. The electrical properties of PST films at microwaves frequencies are very attractive for tunable devices applications because its relatively low perovskite phase formation temperature is compatible with silicon integrated circuits.

In conclusion, we have demonstrated the potential of PST films, directly deposited on high resistivity silicon, for tunable capacitance at microwave frequencies up to 60 GHz. The thermal budget is relatively low and the processing is largely compatible with silicon integrated circuits. The tunability

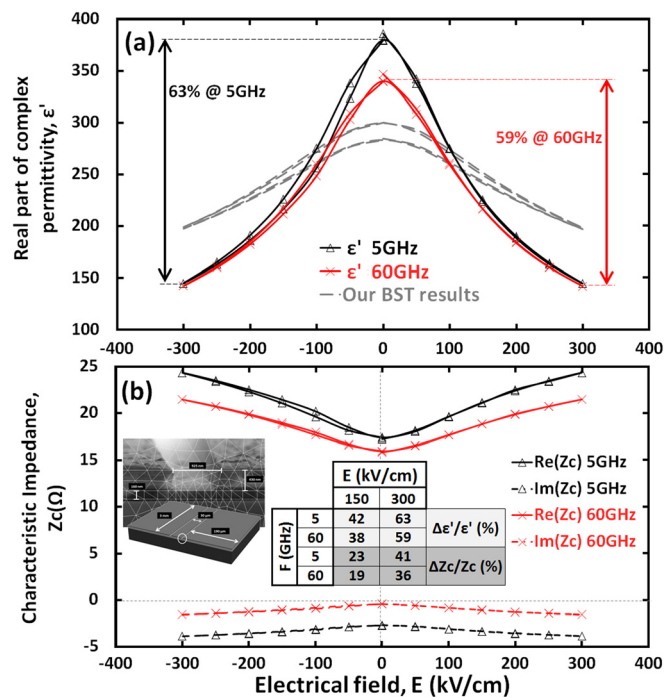


FIG. 4. (Color online) (a) Electrical field dependence at 5 GHz (black line) and at 60 GHz (grey line) of ϵ' for PST thin films deposited on a 600 μm HRSi substrate and (b): The impact of the dielectric PST layer tunability on the structure's characteristic impedance.

reaches a maximum value 59% at 60 GHz in comparison to 29% for BST films at the same frequency. Despite slightly larger dielectric losses, PST thin films achieve a better FOM than BST. These results confirm the potentialities of PST films for the realization of tunable devices at micro waves frequencies. The resonant absorption peaks of the frequency dependent loss tangent, probably in relation with the PST thin film thickness, can be exploited for the fabrication of tunable thin film bulk acoustic wave resonators. In future work, we try to optimize the PST film crystallisation by the introducing a buffer layer (TiO_x or other) and determine the precise relation between the resonant absorption peaks and the film thickness. We will verify that the observed resonant effect is not limited to PST material but must appear also with BST.

¹D. Dimos and C. H. Mueller, *Annu. Rev. Mater. Sci.* **28**, 397 (1998).

²G. Houzet, L. Burgnies, G. Velu, J. C. Carru, and D. Lippens, *Appl. Phys. Lett.* **93**, 053507 (2008).

³F. Ponchel, J. Midy, J. F. Legier, C. Soyer, D. Rémiens, T. Lasri, and G. Guéguan, *J. Appl. Phys.* **107**, 054112 (2010).

⁴J. Zhai, X. Yao, Z. Xu, and H. Chen, *J. Appl. Phys.* **100**, 034108 (2006).

⁵Y. Lin, X. Chen, S. W. Liu, C. L. Chen, J. S. Lee, Y. Li, Q. X. Jia, and A. S. Bhalla, *Appl. Phys. Lett.* **84**, 577 (2004).

⁶X. Lei, D. Remiens, F. Ponchel, C. Soyer, G. Wang, and X. Dong, "Optimization of PST Thin Films Grown by Sputtering and Complete Dielectric Performance Evaluation: An Alternative Material for Tunable Devices," *J. Am. Ceram. Soc.* (to be published).

⁷L. Yang, G. Wang, D. Rémiens, and X. Dong, *J. Am. Ceram. Soc.* **93**(5) 1215 (2010).

⁸F. Ponchel, J.-F. Legier, C. Soyer, D. Rémiens, J. Midy, T. Lasri, and G. Guéguan, *Appl. Phys. Lett.* **96**, 1 (2010).

⁹P. K. Petrov, N. M. Alford, and S. Gevorgyan, *Meas. Sci. Technol.* **16**, 583 (2005).

¹⁰S. Tappe, U. Böttger, and R. Waser, *Appl. Phys. Lett.* **85**(426), 624 (2004).

¹¹K. M. Lakin, G. R. Kline, and K. T. McCarron, *IEEE Trans. Microwave Theory Tech.* **43**, 2933 (1995).